STIM1 and STIM2 protein deficiency in T lymphocytes underlies development of the exocrine gland autoimmune disease, Sjögren's syndrome

Kwong Tai Cheng[a], Ilias Alevizos[b], Xibao Liu[a], Wiliam D. Swaim[a], Hongen Yin[c], Stefan Feske[d], Masatsugu Oh-hora[e,f,g], and Indu S. Ambudkar[a,1]

[a]Secretory Physiology Section, [b]Sjögren's Syndrome Clinic, and [c]AAV Biology Unit, Molecular Physiology and Therapeutic Branch, National Institute of Dental and Craniofacial Research, National Institutes of Health, Bethesda, MD 20892; [d]Department of Pathology, New York University Langone Medical Center, New York, NY 10016; [e]Global Center of Excellence Program, International Research Center for Molecular Science in Tooth and Bone Diseases and [f]Department of Cell Signaling, Graduate School of Medical and Dental Sciences, Tokyo Medical and Dental University, Tokyo 113-8549, Japan; and [g]Japan Science and Technology Agency (JST), Precursory Research for Embryonic Science and Technology (PRESTO) program, Tokyo 113-8549, Japan

Primary Sjögren's Syndrome (pSS) is an autoimmune disease involving salivary and other exocrine glands that leads to progressive lymphocytic infiltration into the gland, tissue damage, and secretory defects. The mechanism underlying this disease remains poorly understood. Here we report that mice with T-cell–targeted deletion of Stromal Interaction Molecule (STIM) 1 and STIM2 [double-knockout (DKO)] mice develop spontaneous and severe pSS-like autoimmune disease, displaying major hallmarks of the disease. In DKO mice, diffuse lymphocytic infiltration was seen in submandibular glands, a major target of pSS, by age 6 wk, progressing to severe inflammation by age 12 wk. Sjögren's syndrome-specific autoantibodies (SSA/Ro and SSB/La) were detected in the serum, and progressive salivary gland destruction and loss of fluid secretion were also seen. Importantly, we report that peripheral blood mononuclear cells as well as lymphocytic infiltrates in submandibular glands from patients with pSS demonstrated significant reductions in STIM1 and STIM2 proteins. Store-operated calcium entry was also reduced in peripheral blood mononuclear cells from pSS patients compared with those from healthy controls. Thus, deficiency of STIM1 and STIM2 proteins in T cells, and consequent defects in Ca^{2+} signaling, are associated with salivary gland autoimmunopathy in DKO mice and pSS patients. These data reveal a previously unreported link between STIM1 and STIM2 proteins and pSS.

immunology | knockout mice | Orai1 | rheumatology

Store-operated calcium entry (SOCE) is activated in response to agonist-stimulated depletion of the endoplasmic reticulum Ca^{2+} store and provides critical cytosolic Ca^{2+} signals that determine the regulation of diverse cellular functions (1). In T lymphocytes, SOCE is mediated by calcium release-activated calcium (CRAC) channels and regulates T-cell activation and function, as well as long-term responses such as gene expression (2–5). Two key components of CRAC channels are stromal interaction molecule (STIM) 1, STIM2, Orai1, Orai2, and Orai3. STIM1 is the primary regulator of SOCE that senses endoplasmic reticulum $[Ca^{2+}]$ and triggers channel activation on store depletion (6, 7). STIM2 is considered a relatively poor activator of SOCE, although it has not yet been fully characterized (5, 8). Orai1, the pore-forming subunit of CRAC channels (9), is the critical component for SOCE in T lymphocytes and other cell types (2, 3, 8, 10).

In humans, disruption of SOCE has major immunologic consequences. Although complete loss of Orai1 function results in the severe combined immune deficiency (SCID) phenotype, patients with mutations in STIM1 display autoimmunity and lymphoproliferation (11). The consequences of STIM2 defects in patients have not yet been reported. Thus, Orai-STIM–dependent Ca^{2+} signaling has a dominant role in the maintenance of immune balance. In a mouse model with T-lymphocyte–targeted deletion

of STIM1 and STIM2, SOCE and SOCE-dependent cytokine production were severely attenuated, along with a substantial decrease in the number and function of regulatory T cells (Tregs) (12). These mice displayed signs of autoimmunity, including dermatitis, blepharitis, and lymphoproliferation, with significant splenomegaly and infiltration of lymphocytes into epithelial tissues, such as liver and lungs.

Primary Sjögren's Syndrome (pSS) is a chronic autoimmune disease affecting exocrine glands, primarily salivary and lacrimal glands, resulting in gland destruction, xerostomia (dry mouth), and keratoconjunctivitis sicca (dry eyes) (13). Extraglandular manifestations such as arthritis, fatigue, and vasculitis, and an elevated incidence of non-Hodgkin lymphoma have been reported as well (14). The current criteria for diagnosis of pSS include subjective and objective signs of dry mouth and/or dry eyes, the presence of anti-Ro/anti-La autoantibodies, and histological evaluation of leukocyte infiltration in the minor salivary gland (MSG); the number of foci of infiltrate in a given area of tissue is graded as 0–12. Although many studies suggest a role for viral infections as well as various extrinsic factors as potential triggers, there are no conclusive data establishing the molecular basis for the disease (15, 16). The late disease onset and the diverse genetic background of affected individuals complicate study of the disease mechanism and pathogenesis. Although several mouse models display a pSS-like phenotype (17–21), no single model can perfectly match the full spectrum of pSS observed in humans.

Based on the autoimmune phenotype of the STIM1 and STIM2 double-knockout (DKO) mice and the generation of pSS-like disease in several mouse models with decreased Treg function (19–24), we assessed a possible link between STIM1 and STIM2 deficiency in T cells and autoimmunopathy of the salivary glands. Here we report that DKO mice display spontaneous and progressive submandibular gland inflammation (within 3 mo), comparable to that seen in pSS patients with severe salivary gland damage. The mice display all of the major hallmarks of pSS: damaged salivary glands, loss of stimulated fluid secretion, and elevated pSS-specific autoantibodies. More importantly, we report that peripheral blood mononuclear cells (PBMCs) from

pSS patients exhibit decreased levels of STIM1 and STIM2 proteins, as well as diminished SOCE. Taken together, these findings suggest that STIM1 and STIM2 deficiencies in T cells, and the consequent aberrations in T cell function, underlies the onset and progression of salivary gland autoimmunopathy in Sjögren's syndrome.

Results

Reduction of Salivary Gland Function in DKO Mice. Saliva secretion was induced by treatment of DKO and control (CTRL) mice with the muscarinic receptor agonist pilocarpine. Litter-matched mice were used in all of the experiments. At 6 wk after birth, pilocarpine-stimulated saliva was 11.10 ± 1.13 μL/20 min/g body weight in CTRL mice and 7.40 ± 1.80 μL/20 min/g body weight in DKO mice, demonstrating a 33.33% reduction in salivary flow in the latter (Fig. 1 A and C). By 12 wk, DKO mice exhibited a striking 56% reduction in saliva secretion compared with CTRL mice (5.14 ± 1.81 μL/20 min/g body weight vs. 11.76 ± 1.38 μL/20 min/g body weight; $P < 0.01$) (Fig. 1 B and C).

Elevation of pSS-Specific Autoantibodies in DKO Mice. Sjögren's syndrome-A (SSA/Ro) and Sjögren's syndrome-B (SSB/La) are two major autoantibodies used for clinical diagnosis in pSS and characterizing mouse models (25, 26). Here 12-wk-old DKO mice displayed an elevated titer of anti-SSA antibody compared with CTRL mice (3.89 ± 0.20 OD$_{450/540}$ vs. 1.71 ± 0.21 OD$_{450/540}$; $P < 0.01$) (Fig. 2A). Anti-SSB titer remained minimal in 12-wk-old CTRL mice (1.49 ± 0.8 ng/mL), significantly lower than that in DKO mice (33.03 ± 1.53 ng/mL; $P < 0.01$) (Fig. 2B). These significant results demonstrate that T-cell–specific deletion of STIM1 and STIM2 leads to generation of pSS-specific autoantibodies in the serum. Combined with the loss of salivary gland function, these findings reveal the onset of salivary gland autoimmunopathy in the DKO mouse model.

Progressive Lymphocytic Infiltration in the Submandibular Glands of DKO Mice. A major diagnostic criterion for pSS is lymphocytic infiltration in the submandibular gland, often the main target in this disease. Fig. 3 shows histological findings in the glands from DKO and CTRL mice. Compared with the morphology of the glands from CTRL mice, moderate levels of infiltrating cells were detected in samples of glands from 6-wk-old DKO mice, which progressed to very severe inflammation by 12 wk. At this stage, there was marked lymphocytic infiltration (arrows), with multiple periductular foci, along with severe destruction of acinar structures. The progress of infiltration was reminiscent of that in patients diagnosed with severe pSS (Fig. 3). A lower-magnification image of the entire gland area (Fig. S1) shows a progressive decrease in healthy glandular tissue and increase in
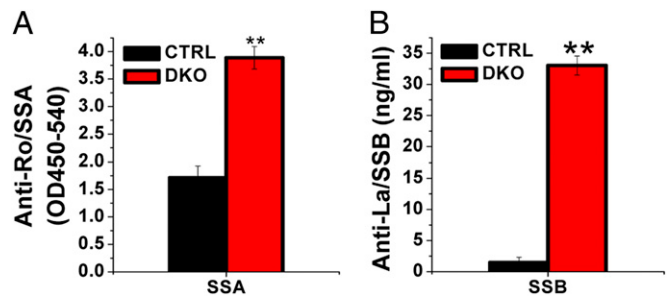

Fig. 2. Detection of pSS-associated autoantibodies in serum. Serum samples were collected from CTRL and DKO mice, and autoantibody levels were measured as described in *SI Materials and Methods* using samples collected at 12 wk and compared between CTRL mice (black) and DKO mice (red). Antibody levels for SSA/Ro (CTRL, 1.71 ± 0.80 OD$_{450/540}$ vs. DKO, 3.89 ± 0.20 OD$_{450/540}$) (A) and SSB/La (CTRL, 1.49 ± 0.80 ng/mL vs. 33.03 ± 1.53 ng/mL) (B) are shown. Data are mean $\pm$ SD. Significant differences are shown; **$P < 0.01$, unpaired Student t test.

diffuse infiltrates. Note that inflammation was not detected in parotid glands visible within the field.

To evaluate the progress of lymphocytic infiltration in DKO mice, the focal infiltrations of inflammatory cells within the salivary gland from different age groups were measured (Fig. S2). The focus score (FS; foci, ≥ 50 cells per 4 mm^2 of tissue) of 6-wk-old DKO mice (2.75 ± 0.96) was comparable to mild/moderate pSS histopathology, whereas the number of infiltrates increased dramatically by 12 wk (11.5 ± 0.71), resembling severe salivary gland inflammation in pSS patients.

Lymphocytic Infiltration and Destruction of Salivary Gland Structure in DKO Mice. The localization of specific markers for acinar cells, epithelial cells, and lymphocytes was examined in sections of submandibular glands from DKO and CTRL mice. In samples from CTRL mice, aquaporin 5 (AQP5; the primary water channel in the gland and marker for acinar cells) showed normal apical localization in the 6-wk and 12-wk groups (the latter shown in Fig. 4A). A normal ductal staining pattern of keratin (epithelial marker) as well as basal and lateral localization of STIM1 was detected in CTRL mouse tissue, whereas CD3 (lymphocyte marker) was not detected. Glands from 6-wk-old DKO mice showed no significant change in the localization of AQP5, keratin, and STIM1, although some CD3 signal was detected in the tissue (Fig. 4B and Figs. S3 and S4). By 12 wk, DKO mice gland displayed severe inflammation. AQP5 (red arrows) was very poorly detected in most of the gland and did not show the typical pattern of localization in the apical region of acini (Fig. 4C and Fig. S5). Residual healthy tissue within the gland
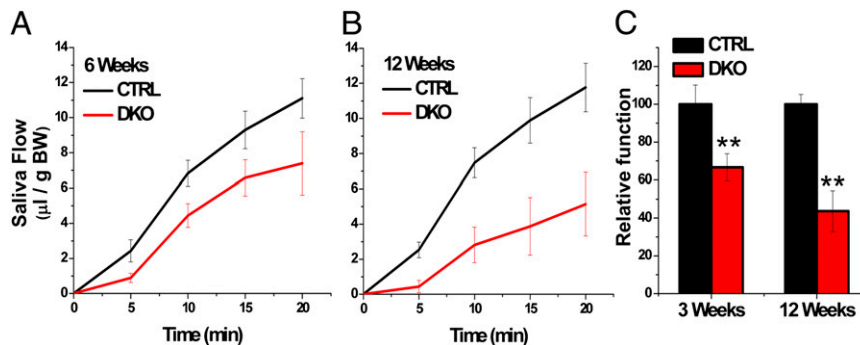

Fig. 1. Salivary gland function is decreased in STIM1 and STIM2 DKO mice. (A and B) Pilocarpine-stimulated saliva flow in CTRL (black) and DKO (red) mice at 6 wk (CTRL, 11.10 ± 1.13 vs. DKO, 7.40 ± 1.80 μL/20 min/g of birth weight) (A) and 12 wk (CTRL 11.76 ± 1.38 vs. DKO 5.14 ± 1.81 μL/20 min/g of birth weight) (B). (C) Average total saliva secretion, with values normalized by body weight. Data are mean value $\pm$ SEM in each group. **$P < 0.01$.

Mouse salivary gland
12 wk CTRL

3 wk DKO

6 wk DKO

12 wk DKO

pSS-salivary gland
Normal
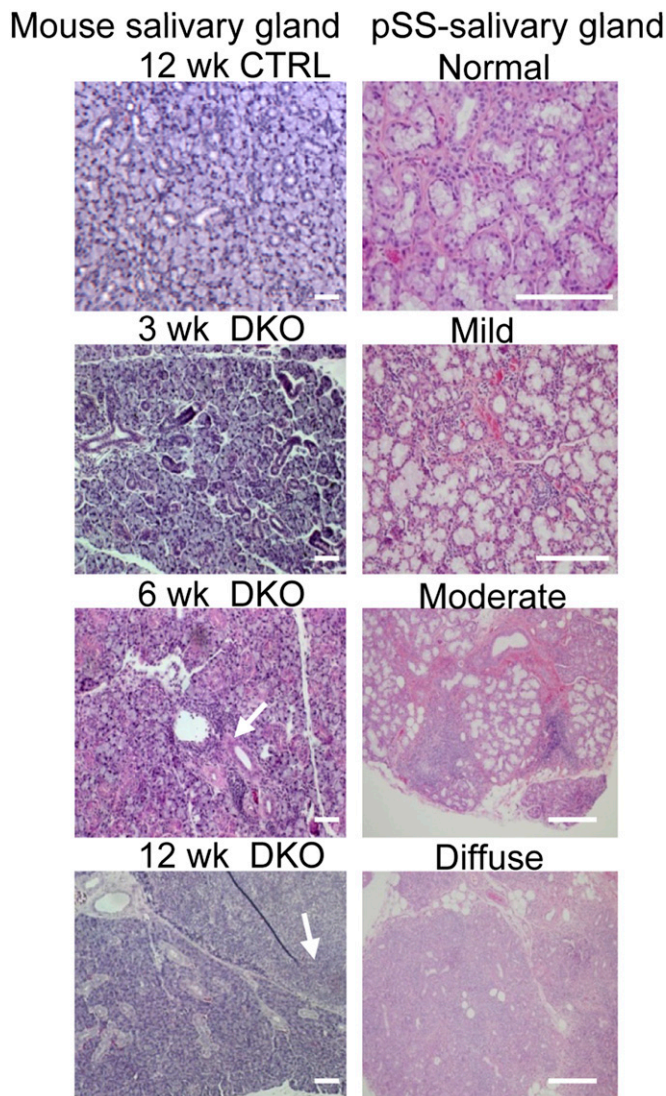
Mild

Moderate

Diffuse

Fig. 3. Morphology of submandibular glands from DKO mice. (Left) H&E stains of the submandibular gland sections from CTRL and DKO mice (original magnification 20×) at various ages as indicated. Arrows indicate infiltrates within the exocrine tissue. (Right) Representative histopathology of MSG samples from pSS patients with increasing severity of disease, with normal to severe (diffuse) infiltration. (Scale bars: 100 μm.)

displayed normal pattern of the protein (Fig. S5, red arrow, white areas indicate disrupted morphology). Similarly keratin, was poorly detected in samples from 12-wk-DKO mice (Fig. 4C), whereas STIM1 staining was detected in disrupted salivary gland structures that appeared to be remnants of ducts and acini (Fig. 4C, red arrows). Interestingly, low-magnification images (Fig. S5) revealed relatively large areas that appeared to be STIM1-negative (white arrow) with normal staining in residual healthy tissue (red arrow). This is to be expected if these represent areas with infiltrating T lymphocytes lacking STIM1 (white arrows). Consistent with this finding, CD3$^+$ cells profusely occupied the damaged (white arrow), but not residual healthy areas of salivary glands from DKO mice (Fig. 4C, red arrow and Fig. S5). Taken together, these data demonstrate progressive infiltration of STIM1- and STIM2-depleted lymphocytes into submandibular glands of DKO mice along with destruction of the salivary gland structure. It should be noted that DKO mice have been reported to have a lymphadenopathy phenotype. However, the detection of AQP5 and keratin within the

inflamed gland rules out the possibility that this extensively inflamed tissue is an enlarged lymphoid organ. In aggregate, our findings demonstrate that the DKO mice display all major hallmarks of pSS and thus can serve as a relevant model for studying the pathogenesis of pSS.

T-Lymphocyte Infiltration in Salivary Gland from pSS Patients. Based on the foregoing findings, we examined STIM1 and CD3 expression in human MSG biopsy specimens acquired from pSS patients with either high FS or low FS. MSG specimens and cervical lymph node sections from healthy volunteers were used as controls. In all of the low-FS MSG biopsy samples tested, normal and relatively strong STIM1 labeling was seen in acinar as well as ductal structures together with low frequency of CD3$^+$ T lymphocytes (Fig. 5A; compare with STIM1 and CD3$^+$ signals detected in 6-wk-old DKO mice). In contrast, most of the high-FS MSGs samples tested showed a clear reduction of STIM1 expression in the infiltrating cells as well as in the residual salivary gland structures, along with a much higher frequency of CD3$^+$ cells within the salivary tissue (Fig. 5B), a pattern reminiscent of that seen in glands from 12-wk-old DKO mice (Fig. S6 provides enlarged areas of these images, and Fig. S7 shows DIC images). STIM1 expression in MSG specimens from high-FS patients appeared to be lower than that in samples from healthy volunteers and low-FS pSS patients (Fig. S8; lymph node was used as a control for STIM1). These data suggest diminished STIM1 in infiltrating T lymphocytes in salivary glands of pSS patients. This intriguing finding suggests that defects in the STIM proteins in T cells might be associated with pSS.

Reduction of STIM1 and STIM2 Expression in PBMCs from pSS Patients. To further evaluate STIM1 and STIM2 involvement in pSS, PBMCs from 17 healthy volunteers (HVs; 15 females, 2 males) and 27 pSS patients (all females) were evaluated by Western blot analysis. Our important findings demonstrate that PBMCs from pSS patients show a >70% reduction in the levels of STIM1 (Fig. 6 A and B) and STIM2 (Fig. 6 A and D)
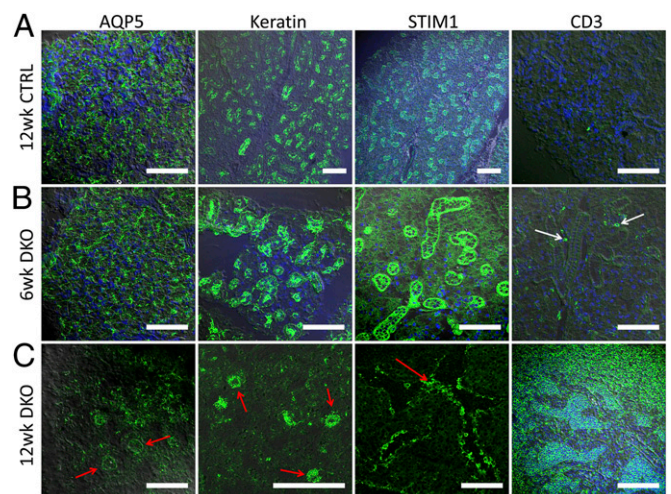

Fig. 4. Expression of salivary gland marker proteins in submandibular glands from control and DKO mice. Immunostaining of submandibular gland tissue obtained from 12-wk-old control mice (A), 6-wk-old DKO mice (B), and 12-wk-old DKO mice (C) indicating localization of AQP5, keratin, STIM1, and CD3 within the gland. White arrows indicate infiltrates within the salivary gland tissue; red arrows indicate the regions where salivary gland/epithelial cell markers are detected. Images shown are 40× overlaid with DIC. (Scale bars: 100 μm.) Enlarged areas of the images are provided in Fig. S3, DIC images are provided in Fig. S4, and 10× and 20× images of the 12-wk-old DKO mouse glands are shown in Fig. S5.
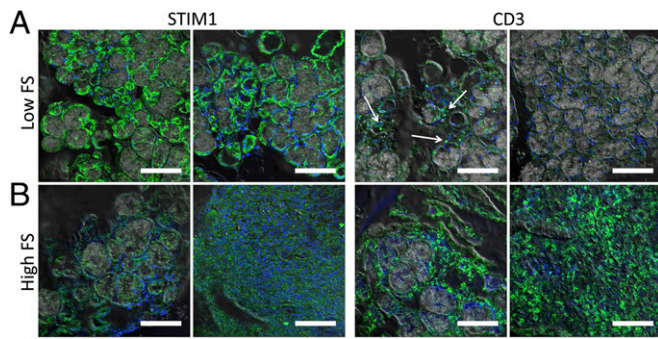
Cheng et al.

Fig. 5. Lymphocytic infiltration and loss of STIM1 expression in MSG biopsy specimens obtained from pSS patients with high FS and low FS. Immunofluorescence images are overlaid with DIC images showing the expression pattern of STIM1 and T-cell marker CD3 (white arrow) in MSG biopsy specimens from pSS patients with low FS (*A*) and high FS (*B*). In *B*, the *Left* panels for both STIM1 and CD3 show staining in residual healthy areas of the gland (some ductal and acinar structure is retained), and the *Right* panels show infiltrated areas. (Scale bars: 100 μm.) Enlarged areas of the images are shown in Figs. S6 and S7, and DIC images of the areas shown in *A* and *B* are provided in Fig. S7.

compared with PBMCs from healthy volunteers. In addition, we show that the decreases in STIM:CD3 and STIM2:CD3 ratios are related to the severity of infiltration, with greater decreases in proteins in PBMCs of patients with moderate to severe infiltrates (FS 4–12) in the salivary glands compared with those with low infiltration (FS 0–3; Fig. 6 *C* and *E*); HVs with low FS are included in the latter group. Note that there was more variability among the samples in the latter group. These findings demonstrate that both STIM1 and STIM2 are disrupted in lymphocytes from pSS patients (consistent the onset of pSS in DKO mice). Furthermore, the decrease in STIM1 and STIM2 is more pronounced in PBMCs of patients who have relatively high levels of infiltrates in the gland.

Functional Consequences of Loss of STIM1 and STIM2 in PMBCs from pSS Patients. SOCE was measured in PBMCs after stimulation with thapsigargin (Tg; Fig. 7 *A–C*), or after crosslinking of TCRs with anti-CD3 antibody, with a 10-min preincubation before Ca^{2+} readdition (Fig. 7 *D–F*). Only female subjects were used in this assay. PBMCs from pSS patients showed a 60% reduction (0.48 ± 0.07; $n = 6$) in Tg-mediated Ca^{2+} response (change in 340/380 ratios) compared with those from HVs (1.26 ± 0.07; $n = 4$) (Fig. 7 *A* and *B*). Anti-CD3–induced Ca^{2+} influx was also reduced by 44% in pSS PBMCs (0.33 ± 0.04; $n = 3$) compared with that in cells from HVs (0.59 ± 0.02; $n = 4$) (Fig. 7 *D* and *E*). Both the amplitude and initial rates of Ca^{2+} influx were decreased significantly in PBMCs from pSS (Fig. 7 *C* and *F*). These results collectively provide evidence that reduction in STIM1 and STIM2 protein expression in T lymphocytes leads to a compromise in their function that could contribute to the onset and progression of pSS-induced autoimmune exocrinopathy.

Discussion

pSS is an autoimmune disease that leads to persistent and progressive inflammation of exocrine glands, such as salivary and lacrimal glands, resulting in tissue damage and loss of function. The mechanism(s) underlying the pathogenesis of pSS is poorly understood despite the relatively high prevalence of the disease. Here we report an association between STIM1 and STIM2 deficiency in T lymphocytes and autoimmunopathy of salivary glands. Our findings demonstrate that T-cell–specific ablation of STIM1 and STIM2 in mice leads to the development of severe Sjögren's syndrome–like exocrinopathy and the following key features of pSS: progressive loss of salivary fluid secretion,

elevation of Sjögren-specific autoantibodies SSA and SSB in the serum, progressive lymphocytic infiltration in the submandibular gland starting at 6 wk after birth and progressively worsening by 12 wk, and substantial disruption of salivary gland tissue. The severity of the inflammation in 3-mo-old animals was similar to that seen in pSS patients with severe inflammation. Thus, loss of STIM1 and STIM2 expression in T cells of mice led to onset and progression of pSS-like disease, suggesting a potential role for STIM proteins and T-cell function in the pathogenesis of Sjögren's syndrome. These findings also establish DKO mice as a suitable model for studying the pathogenesis of pSS.

A key finding of this study is that lymphocytes infiltrating salivary gland as well as PBMCs obtained from pSS patients exhibit drastic diminished STIM1 and STIM2 expression. Importantly, the STIM1 and STIM2 deficiency in PBMCs was physiologically relevant and led to reduced SOCE in T cells. Although decreased STIM1 expression in other lymphocyte subsets may contribute to the disease process, the data obtained from our studies with DKO mice and pSS patients suggest that the dysregulation of STIM proteins and SOCE in T lymphocytes could underlie the pathogenesis of Sjögren's syndrome. Our findings are in agreement with recent studies reporting complex immunologic symptoms and premature death in patients lacking functional STIM1; key clinical features include immunodeficiency, lymphoproliferation, and autoimmunity (8, 11). Although the immunodeficiency is a direct result of severely
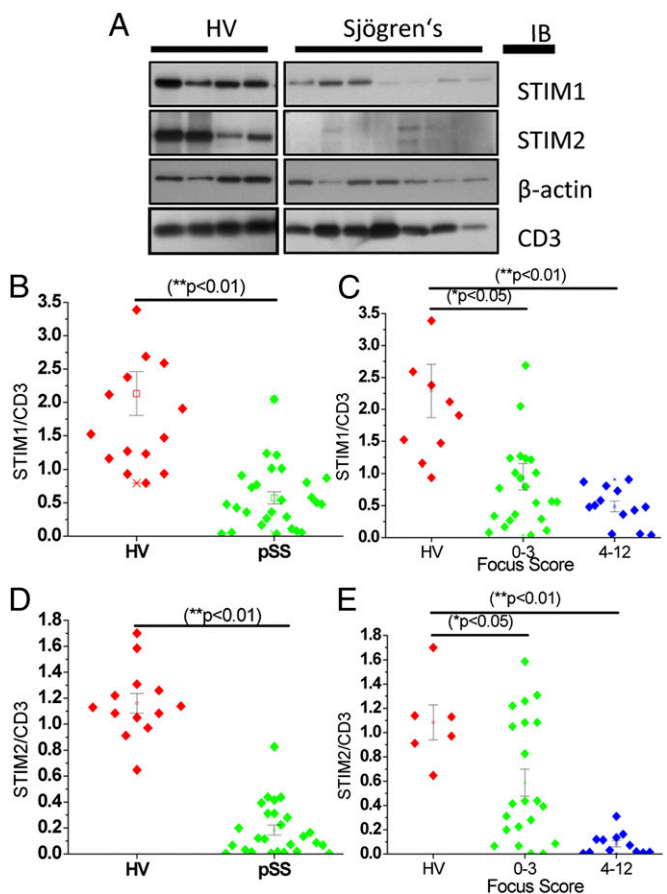

Fig. 6. Reduced STIM1 and STIM2 protein expression in pSS PBMCs. (*A*) Representative Western blot showing STIM1 and STIM2 expression in PBMCs from HVs and patients with pSS. (*B* and *D*) Relative expression of STIM1 and STIM2 normalized to CD3 in PBMCs from 17 HVs and 27 pSS patients. *P < 0.01. (*C* and *E*) Relative expression of STIM1 and STIM2 in PBMCs (normalized to CD3) shown as a function of FS (0–3 or 4–12, with 0 being no inflammation and 12 the greatest inflammation). *P < 0.05; **P < 0.01.

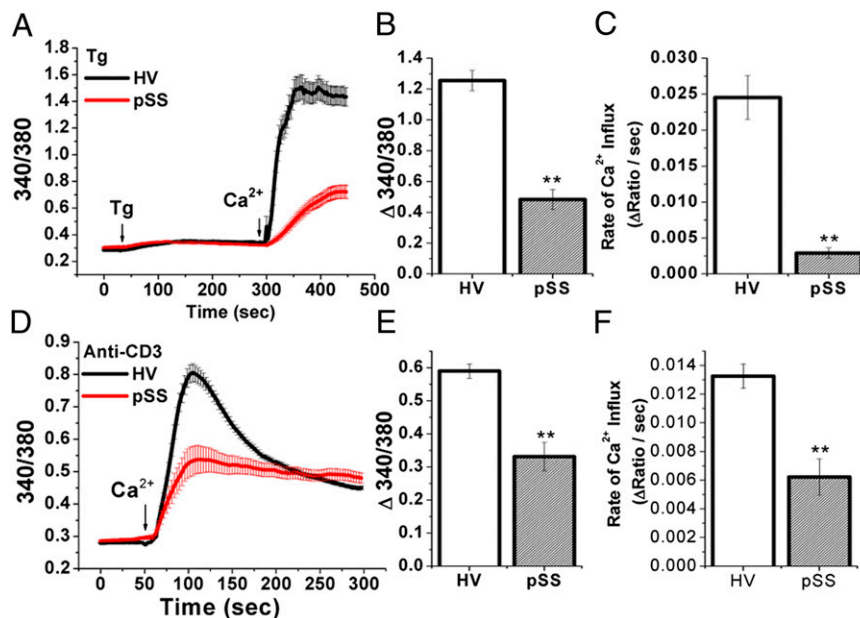IMMUNOLOGY

Fig. 7. Impaired store-operated Ca^{2+} entry in pSS PBMCs. Ca^{2+} entry in PBMCs after stimulation with thapsigargin (*A–C*) or anti-CD3 antibody (*D–F*), with cells preincubated with anti-CD3 for 10 min in Ca^{2+}-free medium before the start of the trace. *A* and *D* show average Ca^{2+} influx responses in PBMCs from an HV (black) and a pSS patient (red). *B* and *E* show the average Ca^{2+} influx amplitude (fluorescence increase after Ca^{2+} addition). In each case, resting fluorescence was subtracted from the peak 340/380 ratio (Tg: HV, 1.26 ± 0.07 vs. pSS, 0.48 ± 0.07; CD3: HV, 0.59 ± 0.02 vs. pSS, 0.33 ± 0.04). *C* and *F* show the average rate of Ca^{2+} influx, the rate of fluorescence increase after Ca^{2+} addition (Tg: HV, 0.0245 ± 0.003 vs. pSS, 0.0029 ± 0.001; CD3: HV, 0.0132 ± 0.001 vs. pSS, 0.006 ± 0.001). Error bars represent SEM. **Values significantly different ($P < 0.01$) from the respective control value. Data represent results from at least 50–150 cells for each group.

impaired T-cell activation, morbidity in most cases is related to recurrent pathogenic infections. It has been suggested that the lymphoproliferation and autoimmunity exhibited by these patients are mainly associated with a decrease in Treg population (27). Maintenance of the STIM-Orai–dependent SOCE as well as specific cell functions regulated downstream from SOCE, such as cytokine production, is crucial for normal immune homeostasis, especially as governs Treg differentiation. Studies in mice have also led to similar conclusions. Whereas global deletion of Orai1, STIM1, or STIM2 in mice results in premature death (12, 28, 29), T-cell–targeted deletion of both STIM1 and STIM2 leads to autoimmune symptoms. Decreased numbers of Tregs as well as compromised suppressive function of Tregs on effector T cells were noted in these mice, suggesting that Treg development appears to be especially sensitive to the absence of STIM-dependent Ca^{2+} influx (12). It also has been demonstrated that calcineurin-NFAT signaling, which is activated by Ca^{2+} entry via SOCE channels, is important for regulating Treg development and function (30, 31). Thus, compromise of SOCE in T lymphocytes could be a causative factor.

It is also important to consider the distinct clinical phenotypes that are induced by intrinsic genetic mutation of STIM or somatic dysregulation of STIM. Conditions that result in ablation of STIM expression or function result in complete compromise of T-cell development, and patients expressing such mutations (or global KO in mice) have severe immunodeficiency and a poor survival rate. In contrast, STIM expression can be altered at a relatively late stage in the T-cell cycle. In the T-cell–targeted DKO mice, homozygous gene deletion does not occur until the double-positive stage in the T-cell life cycle. Thus, the residue protein can support Ca^{2+} entry in the early stage of T-cell development and only later processes (e.g., Treg differentiation) are affected. This could explain the different phenotypes seen after STIM1 KO vs. targeted T-cell KO of STIM1 and STIM2 in mice; the former induces lethality, whereas in the latter is

associated with normal thymic development but compromised Treg differentiation (12). These observations suggest that attenuation of the STIM signaling pathway in various stage of the T-cell life cycle can lead to different fates of T lymphocytes and immune homeostasis. Such delayed effects in the T-cell cycle can also account for the heterogeneity and late disease onset of Sjögren's syndrome. We have not yet determined how exactly STIM protein levels are modulated in exocrine gland and lymphocytes in pSS patients. Possibly exocrine, endocrine, or other factors, such as miRNA, transcriptional dysregulation, or viral infections, could trigger mechanisms that result in reduced STIM proteins in these cells (32, 33).

A number of studies in human and animal models have revealed the potential involvement of Treg dysregulation in SS pathogenesis. Synthesis of IL-2, a critical factor in Treg differentiation and activation, in T cells is dependent on activation of NFAT by SOCE (34). NOD mice, a frequently used mouse model for pSS, display a reduction in IL-2 together with an age-dependent reduction in Treg population and onset of SS (23, 24, 35). IL-2 KO and IL-2Rα KO mice, which exhibit deficient Treg populations, develop severe lymphocyte infiltration in the salivary and lacrimal glands with decreased secretory function (21, 22). Furthermore, mice with T-cell–specific deletion of class 1A phosphoinositide 3-kinase, which develop SS-like autoimmunity, display reduced IL-2 activity and decreased Treg populations (19). TGF-β is another critical regulator of Treg proliferation and function (36); mice lacking TGF-β1 develop an autoimmune disorder resembling human pSS (37). Consistent with the findings in mouse models, two studies of pSS patients demonstrated reduced Treg numbers in salivary glands (38) as well as PBMCs (38, 39). However, a recent report of an STIM1-deficient patient suggested that intrinsic defects in other immune cell populations, such as natural killer cells, natural killer T cells, and B cells, could also contribute to the complex clinical phenotype seen in patients with STIM1 deficiency (40). This is consistent with studies in mice

Cheng et al.

showing that B-cell knockdown of STIM1 and STIM2 led to exacerbation of experimental autoimmune encephalomyelitis, suggesting STIM-dependent SOC influx as a key signal for B-cell regulatory function required to limit autoimmunity (41). Thus, far, STIM2 defects or mutations have not been reported in any clinical conditions. Moreover, the physiological function of STIM2 in immune cells has not yet been established.

In aggregate, the data presented here demonstrate a functional link between STIM deficiency in T lymphocytes and progression of the autoimmune exocrine gland disease pSS. Although the possible contribution of other immune cells in the onset and development of pSS cannot be ruled out, we suggest that loss of STIM proteins, and consequent impairment of SOCE in T lymphocytes, could lead to defects in lymphocyte function, cytokine production, and possibly compromised development and function of Tregs. Further studies are needed to delineate the mechanism (s) by which STIM1 and STIM2 expression in T lymphocytes is

modulated, which might be a critical factor in disease development. In conclusion, this study suggests an important role for STIM proteins in the molecular mechanism underlying pathogenesis of Sjögren's syndrome.

Materials and Methods

All reagents and detailed methods are described in *SI Materials and Methods*. These include saliva collection, cell preparation, calcium imaging, and all biochemical and morphological techniques. Descriptions of animals used, as well as patient samples, are also provided in *SI Materials and Methods.*

1. Putney JW, Jr. (1986) A model for receptor-regulated calcium entry. *Cell Calcium* 7: 1–12.
2. Lewis RS (2001) Calcium signaling mechanisms in T lymphocytes. *Annu Rev Immunol* 19:497–521.
3. Feske S (2007) Calcium signalling in lymphocyte activation and disease. *Nat Rev Immunol* 7:690–702.
4. Hogan PG, Rao A (2007) Dissecting ICRAC, a store-operated calcium current. *Trends Biochem Sci* 32:235–245.
5. Oh-hora M, Rao A (2008) Calcium signaling in lymphocytes. *Curr Opin Immunol* 20:250–258.
6. Zhang SL, et al. (2005) STIM1 is a Ca²⁺ sensor that activates CRAC channels and migrates from the Ca²⁺ store to the plasma membrane. *Nature* 437:902–905.
7. Liou J, Fivaz M, Inoue T, Meyer T (2007) Live-cell imaging reveals sequential oligomerization and local plasma membrane targeting of stromal interaction molecule 1 after Ca²⁺ store depletion. *Proc Natl Acad Sci USA* 104:9301–9306.
8. Hogan PG, Lewis RS, Rao A (2010) Molecular basis of calcium signaling in lymphocytes: STIM and ORAI. *Annu Rev Immunol* 28:491–533.
9. Feske S, et al. (2006) A mutation in Orai1 causes immune deficiency by abrogating CRAC channel function. *Nature* 441:179–185.
10. Abdullaev IF, et al. (2008) Stim1 and Orai1 mediate CRAC currents and store-operated calcium entry important for endothelial cell proliferation. *Circ Res* 103:1289–1299.
11. Feske S, Picard C, Fischer A (2010) Immunodeficiency due to mutations in ORAI1 and STIM1. *Clin Immunol* 135:169–182.
12. Oh-Hora M, et al. (2008) Dual functions for the endoplasmic reticulum calcium sensors STIM1 and STIM2 in T cell activation and tolerance. *Nat Immunol* 9:432–443.
13. Delaleu N, Jonsson MV, Appel S, Jonsson R (2008) New concepts in the pathogenesis of Sjögren's syndrome. *Rheum Dis Clin North Am* 34:833–845, vii.
14. Theander E, et al. (2006) Lymphoma and other malignancies in primary Sjögren's syndrome: A cohort study on cancer incidence and lymphoma predictors. *Ann Rheum Dis* 65:796–803.
15. Hansen A, Lipsky PE, Dörner T (2005) Immunopathogenesis of primary Sjögren's syndrome: Implications for disease management and therapy. *Curr Opin Rheumatol* 17:558–565.
16. Nikolov NP, Illei GG (2009) Pathogenesis of Sjögren's syndrome. *Curr Opin Rheumatol* 21:465–470.
17. Cha S, Peck AB, Humphreys-Beher MG (2002) Progress in understanding autoimmune exocrinopathy using the non-obese diabetic mouse: An update. *Crit Rev Oral Biol Med* 13:5–16.
18. Delaleu N, Nguyen CQ, Peck AB, Jonsson R (2011) Sjögren's syndrome: studying the disease in mice. *Arthritis Res Ther* 13:217.
19. Oak JS, et al. (2006) Sjögren's syndrome-like disease in mice with T cells lacking class 1A phosphoinositide-3-kinase. *Proc Natl Acad Sci USA* 103:16882–16887.
20. Sharma R, Deshmukh US, Zheng L, Fu SM, Ju ST (2009) X-linked Foxp3 (Scurfy) mutation dominantly inhibits submandibular gland development and inflammation respectively through adaptive and innate immune mechanisms. *J Immunol* 183:3212–3218.
21. Sharma R, et al. (2006) Novel animal models for Sjögren's syndrome: Expression and transfer of salivary gland dysfunction from regulatory T cell-deficient mice. *J Autoimmun* 27:289–296.

22. De Paiva CS, et al. (2010) Age-related T-cell cytokine profile parallels corneal disease severity in Sjögren's syndrome-like keratoconjunctivitis sicca in CD25KO mice. *Rheumatology (Oxford)* 49:246–258.
23. Salam MA, et al. (2004) E2f1 mutation induces early onset of diabetes and Sjögren's syndrome in nonobese diabetic mice. *J Immunol* 173:4908–4918.
24. Tang Q, et al. (2008) Central role of defective interleukin-2 production in the triggering of islet autoimmune destruction. *Immunity* 28:687–697.
25. Wahren M, Skarstein K, Blange I, Pettersson I, Jonsson R (1994) MRL/lpr mice produce anti-Ro 52,000 MW antibodies: Detection, analysis of specificity and site of production. *Immunology* 83:9–15.
26. Skarstein K, Wahren M, Zaura E, Hattori M, Jonsson R (1995) Characterization of T cell receptor repertoire and anti-Ro/SSA autoantibodies in relation to sialadenitis of NOD mice. *Autoimmunity* 22:9–16.
27. Picard C, et al. (2009) STIM1 mutation associated with a syndrome of immunodeficiency and autoimmunity. *N Engl J Med* 360:1971–1980.
28. Gwack Y, et al. (2008) Hair loss and defective T- and B-cell function in mice lacking ORAI1. *Mol Cell Biol* 28:5209–5222.
29. Vig M, et al. (2008) Defective mast cell effector functions in mice lacking the CRACM1 pore subunit of store-operated calcium release-activated calcium channels. *Nat Immunol* 9:89–96.
30. Wu Y, et al. (2006) FOXP3 controls regulatory T cell function through cooperation with NFAT. *Cell* 126:375–387.
31. Sakaguchi S, Sakaguchi N (1988) Thymus and autoimmunity. Transplantation of the thymus from cyclosporin A-treated mice causes organ-specific autoimmune disease in athymic nude mice. *J Exp Med* 167:1479–1485.
32. Alevizos I, Illei GG (2010) MicroRNAs as biomarkers in rheumatic diseases. *Nat Rev Rheumatol* 6:391–398.
33. Gallo A, Tandon M, Alevizos I, Illei GG (2012) The majority of microRNAs detectable in serum and saliva is concentrated in exosomes. *PLoS ONE* 7:e30679.
34. McCarl CA, et al. (2010) Store-operated Ca²⁺ entry through ORAI1 is critical for T cell-mediated autoimmunity and allograft rejection. *J Immunol* 185:5845–5858.
35. Anderson JT, Cornelius JG, Jarpe AJ, Winter WE, Peck AB (1993) Insulin-dependent diabetes in the NOD mouse model. II. Beta cell destruction in autoimmune diabetes is a TH2 and not a TH1 mediated event. *Autoimmunity* 15:113–122.
36. Chen W, et al. (2003) Conversion of peripheral CD4⁺CD25⁻ naive T cells to CD4⁺CD25⁺ regulatory T cells by TGF-beta induction of transcription factor Foxp3. *J Exp Med* 198:1875–1886.
37. McCartney-Francis NL, et al. (1996) Autoimmune Sjögren's syndrome-like lesions in salivary glands of TGF-beta1–deficient mice are inhibited by adhesion-blocking peptides. *J Immunol* 157:1306–1312.
38. Li X, et al. (2007) T regulatory cells are markedly diminished in diseased salivary glands of patients with primary Sjögren's syndrome. *J Rheumatol* 34:2438–2445.
39. Liu MF, Lin LH, Weng CT, Weng MY (2008) Decreased CD4+CD25+bright T cells in peripheral blood of patients with primary Sjögren's syndrome. *Lupus* 17:34–39.
40. Fuchs S, et al. (2012) Antiviral and regulatory T cell immunity in a patient with stromal interaction molecule 1 deficiency. *J Immunol* 188:1523–1533.
41. Matsumoto M, et al. (2011) The calcium sensors STIM1 and STIM2 control B cell regulatory function through interleukin-10 production. *Immunity* 34:703–714.

IMMUNOLOGY